JETIR.ORG ISSN: 2349-5162 | ESTD Year : 2014 | Monthly Issue
JOURNAL OF EMERGING TECHNOLOGIES AND INNOVATIVE RESEARCH (JETIR)
An International Scholarly Open Access, Peer-reviewed, Refereed Journal

Radiation Shielding Properties of Some Transition Metal Salts.

Kalidas B. Gaikwad[a*]

[a*]Department of Physics Dr. Babasaheb Ambedkar Marathwada University Chhatrapati Sambhajinagar 431004.
[b]Deogiri College Chhatrapati Sambhajinagar.

Abstract:

This research made use of the radiation shielding properties of some transition metal salts. We used a NaI (Tl) scintillation detector and a variety of gamma-ray sources to investigate the gamma-ray shielding qualities of the manufactured materials. Theoretical values and experimental data showed a remarkable correlation. This software application assessed the effectiveness of manufactured ferrite nanoparticles to shield against gamma radiation. Metal salts have been subjected to gamma radiation from a variety of sources by varying the strength of the radiation dosage. The mass and linear attenuation coefficients, mean free path, half value layer, tenth value layer, and metal salts at 122-1330 keV are studied using XCOM software. Transition Metal Salts are known to enhance γ-radiation shielding.

Keywords: Transition Metal Salts and Radiation shielding parameters.

1. Introduction

Ionizing radiation is a type of energy that has numerous applications in a variety of disciplines, including power generation, healthcare, agriculture, and research [1-6]. Nonetheless, because ionizing radiation has the ability to separate electrons from atoms, it can have a severe deleterious influence on human health [7]. As a result, efficient shielding materials are essential for reducing human exposure to ionizing radiation. Gamma-rays and X-rays are high intensity electromagnetic waves. This type of radiation is employed in a variety of fields, including medicine, nuclear power, and Aerospace industry. Radiation shielding products safeguard anyone working in these industries from radiation exposure. Pb is commonly used for radiation shielding due to its inexpensive cost, high atomic number, and ease of processing. However, it has considerable downsides, such as high toxicity and mass density. Researchers have studied composites with metal particles like barium sulfate ($BaSO_4$) and tungsten oxide (WO_3) mixed with resin or rubber to create Pb-free radiation shielding materials [8-12].

High-atomic-number elements effectively defend against high-energy radiation, including X-rays and gamma-rays. Lead's high density (11.5 g/cm^3) and atomic number (Z = 82) make it a common material for gamma-ray experiments. Protection, particularly in nuclear power plants and medical diagnosis and treatment

facilities.

Lead's severe toxicity requires it to be covered with structural materials like concrete, increasing the thickness of the shielding material. The usage of lead in nuclear shielding is decreasing, with plates constructed of W, Al, Fe, and Cu metals emerging as viable substitutes. Metal plates are used to support concrete constructions, Concrete's strong hydrogen and oxygen content provide neutron protection, whereas plates give gamma protection. Concrete can be supplemented with boron atoms to enhance neutron shielding [13-14].

Because of their high molecular content, oxidized compounds such as ZnO, CuO, Dy2O3, Al2O3, V2O5, SiO2, CdO, SrO, Bi2O3, CoO, and Nd2O3 have been widely explored as gamma-shielding additions in glass composition.

Weight and ability to engage in a glass network structure At the moment, nuclear shielding materials can only protect against particle or photon radiation. Multi-layer radiation shields are commonly used to shield against particle and photon radiation. Multilayer shields guard against neutrons while absorbing gamma rays. Stacking layers results in thick, heavy, and expensive constructions [15-21].

New shielding materials with high gamma-ray attenuation capacity should be investigate, some transitional metal salts like Carbon Monoxide; Molybdenum, Silver, cyanide, Dioxo platinum, Tetrachloroplatinum, Lanthanum (3^+) trichloride, Pentachloro niobium. Transition Metal Salts are expected to have high photon attenuation capacity. For the first time in the literature, the radiation shielding ability of Transition Metal Salts is examined in comparison.

2. Experimental

2.1 Material and method:

To assess the shielding effectiveness of transition metal borides, a variety of elements with moderate to high atomic numbers (Z) were chosen and emphasized in the table 1. Carbon Monoxide Molybdenum(C_6O_6Mo); Silver, cyanide ($CAgN$), Dioxo platinum (O_2Pt), Tetrachloroplatinum(Cl_4Pt), Lanthanum (3^+) trichloride (Cl_3La), Pentachloro niobium (Cl_5Nb). Only chemicals that are thermodynamically stable were chosen. These materials were purchased from Sigma-Aldrich.

2.2 Experimental procedures

Gamma rays from the radioactive sources ^{57}Co, ^{133}Ba, ^{22}Na, ^{137}Cs, ^{54}Mn, and ^{60}Co were used to irradiate the manufactured nanocrystalline spinel ferrites in pellet form using a narrow beam geometry setup and a NaI (Tl) scintillation detector. All of these radioactive sources, which were obtained at the Bhabha Atomic Research Centre (BARC) in Mumbai, India, produced various energy, including ^{57}Co (122 keV), ^{133}Ba (356 keV), ^{22}N (662 keV), ^{54}Mn (835 keV), and ^{60}Co (1173 and 1332 keV). The angle between the radioactive source and the pellet materials was kept at 900 throughout narrow beam analysis.

A NaI (Tl) scintillation detector with narrow beam geometry was employed for gamma ray spectroscopy. The enhanced signals were quantified utilizing spectrometry on a (2" x 2") NaI (Tl) crystal with an energy resolution of 8.2% at 662 keV due to ^{137}Cs gamma decay. A full width at half maximum (FWHM)

and an 8 K multichannel analyzer are required for peak energy versus count measurements [22].**Table 1: Description of the Transition Metal Salts, including their chemical formula, density, molar mass, and Abbreviation.**

Transition Metal Salts	Chemical Formula	Density (g/cm^3)	Molar mass (g/mol)	Abbreviation
Carbon Monoxide; Molybdenum	C_6O_6Mo	1.960	264.02	CM
Silver, cyanide	CAgN	3.943	133.8856	SiC
Dioxo platinum	O_2Pt	10.20	227.08	DPt
Tetrachloroplatinum	Cl_4Pt	4.303	336.9	TClP
Lanthanum (3^+) trichloride	Cl_3La	3.840	245.26	LTCl
Pentachloro niobium	Cl_5Nb	2.750	270.17	PClNb

3. Results and discussion:

To the best of our knowledge, samples of transitional metal salts such as carbon monoxide, molybdenum , silver, cyanide, dioxo platinum, and tetrachloroplatinum were used in this work to generate a good gamma ray material.

3.1 Linear attenuation coefficient (LAC)

Figure 1. clearly shows the linear attenuation coefficient in relation to photon energy for all of the Transition Metal Salts studied. As can be seen, the linear attenuation coefficient for Transition Metal Salts decreases exponentially with increasing photon energy. Dioxo platinum has the highest m value, whilst carbon monoxide and molybdenum have the lowest. Furthermore, carbon monoxide and molybdenum decay more rapidly in the 122 to 356 keV energy range. The linear attenuation coefficient is an important quantity when determining a material's shielding properties. (23)

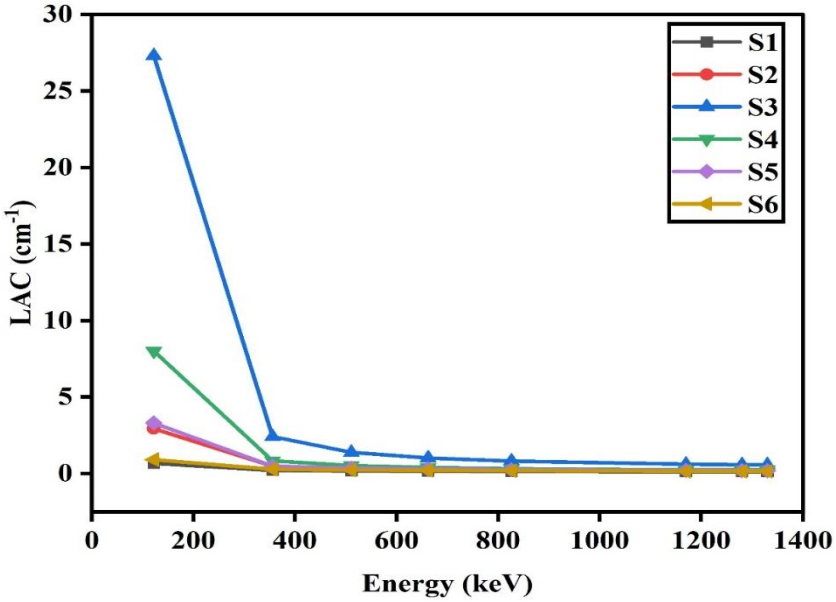

Fig.1. Experimental Linear Attenuation Coefficient (LAC) of Transition Metal Salts

Table 2. The comparison between the experimental and XCOM-MAC values for the Transition Metal Salts under investigation

Energy	Exp	XCOM	Exp	XCOM	Exp	XCOM	Exp	XCOM	Exp	XCOM	Exp	XCOM
122	0.3368	0.3358	0.7454	0.7425	2.6766	2.6650	1.8624	1.8550	0.8601	0.5670	0.3324	0.3314
356	0.1044	0.1058	0.1193	0.1221	0.2282	0.2377	0.1851	0.1919	0.1252	0.1283	0.1022	0.1037
511	0.0867	0.0867	0.0906	0.0906	0.1365	0.1365	0.1190	0.1190	0.0926	0.0926	0.0849	0.0849
662	0.0760	0.0760	0.0765	0.0765	0.1001	0.1000	0.0915	0.0915	0.0771	0.0771	0.0744	0.0744
826	0.0680	0.0675	0.0670	0.0664	0.0802	0.0790	0.0757	0.0747	0.0670	0.06.637	0.0665	0.0660
1170	0.0569	0.0260	0.0549	0.0361	0.0599	0.0467	0.0586	0.0402	0.0546	0.0352	0.0556	0.0294
1280	0.0545	0.0259	0.0525	0.0367	0.0565	0.0479	0.0555	0.0410	0.0521	0.0357	0.0533	0.0295
1330	0.0539	0.0259	0.0520	0.0370	0.0558	0.0485	0.0549	0.0414	0.0516	0.0360	0.0528	0.0296

3.2 Mass attenuation coefficient (MAC)

As shown in Table 2, the experimental design is quite precise and accurate, making it a helpful tool for determining the MAC of various transition metal salts. The comparison between the experimental and XCOM-MAC values for the Transition Metal Salts under investigation

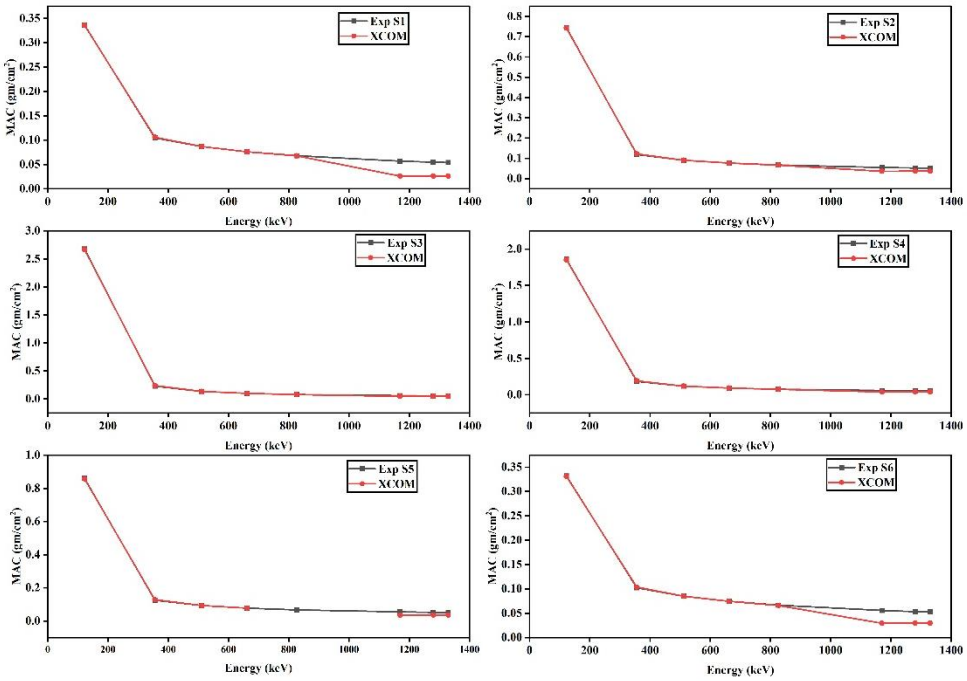

Fig.2. Mass Attenuation Coefficient (MAC) of theoretical and experimental Transition Metal Salts.

Figure 2 shows the results of MAC calculations for gamma rays with energies of 122, 356, 511, 662, 1170, 1275, and 1330 using XCOM software and experimental procedures. This graphic demonstrates that the XCOM software and the experiment data match well. This picture also depicts the MAC's response to incoming gamma-ray energy and how it fluctuates with various energies. This is due to the generally established fact that gamma rays interact with materials in three distinct ways, depending on their energy level [24-26]. The experimental mass attenuation coefficient (MAC) for each of the six Transition Metal Salts was compared to theoretical XCOM Software data as energy increased. Furthermore, Table 2 contains the values for both procedures. Because the experimental MAC results will be used to calculate the other parameters, validating the experimental technique is an important step that this comparison intends to complete. The experimental results are depicted by the black line in the six subfigures, while the theoretical XCOM results are depicted by the red square. Among the tested samples, S3 had higher MAC values than the others[27].

3.3 Mean free path (MFP)

Figure 3 depicts the mean free path (MFP) of produced Transition Metal Salts. Sample S1 has the highest MFP at 1330 keV, while the lowest MFP value is achieved at the lowest measured energy, S3. Higher intensity radiation may easily infiltrate the incident substance, resulting in an upward trend in the MFP [28-29].

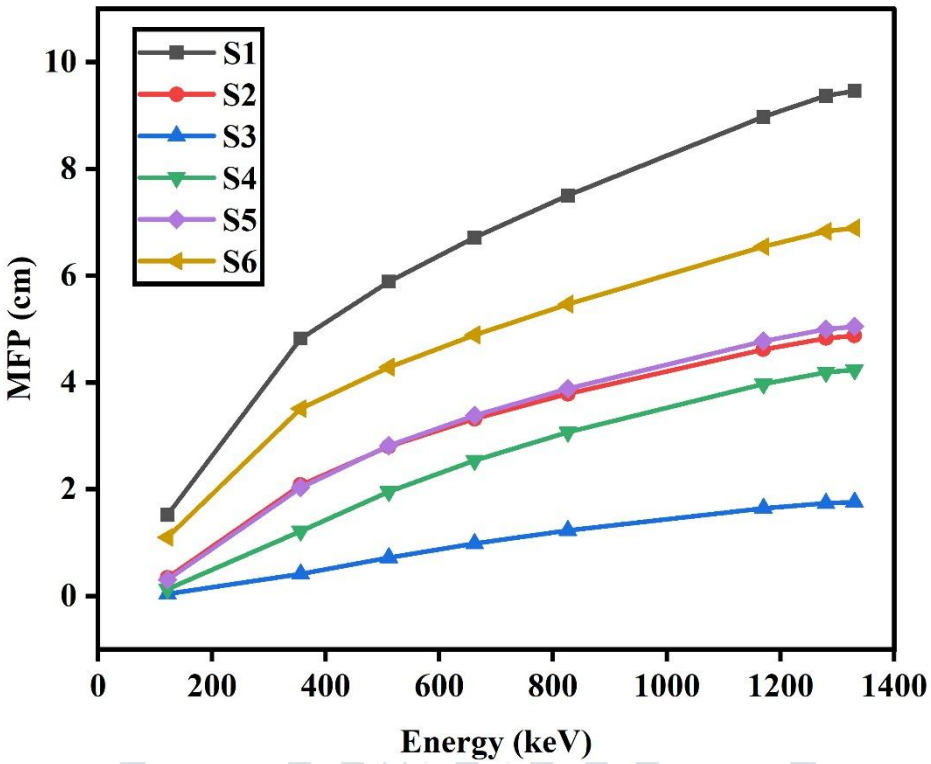

Fig. 3. Mean Free Path (MFP) of Transition Metal Salts.

3.4 Half value layer (HVL) and Tenth value layer (TVL)

Figures 4 and 5 depicted the HVL and TVL results for the prepared samples, respectively. As energy grows, so does the HVL. In other words, the S1 sample has the highest HVL but also the least ideal shielding ability, whereas the S3 sample has the lowest HVL but the finest shielding ability. In addition, the effect of energy on the HVL was investigated. It has been observed that when energy levels increase, so does HVL. The HVL of the S1 sample grew from 1.050 to 3.341 cm at energies of 122, 356, 511, 662, 1170, 1275, and 1330 keV, ranging from 4.079 to 6.556 cm [30-32].

Similarly, in the input photon energy range of 122-1330 keV, experimental values of TVL behave similarly to HVL [33-36].

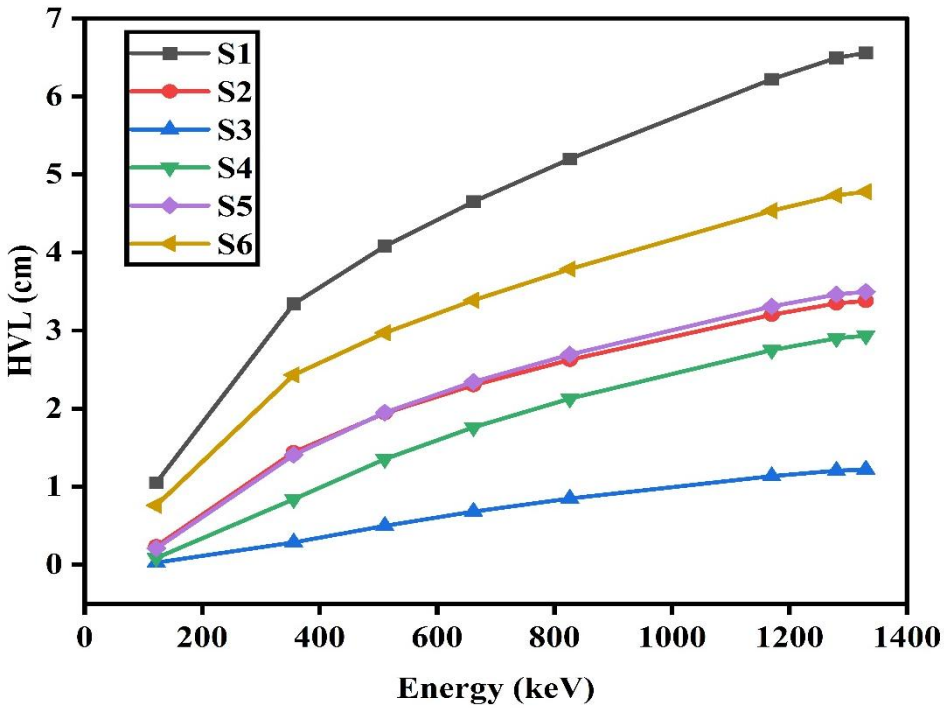

Fig. 4 Half Value Layer (HVL) of Transition Metal Salts.

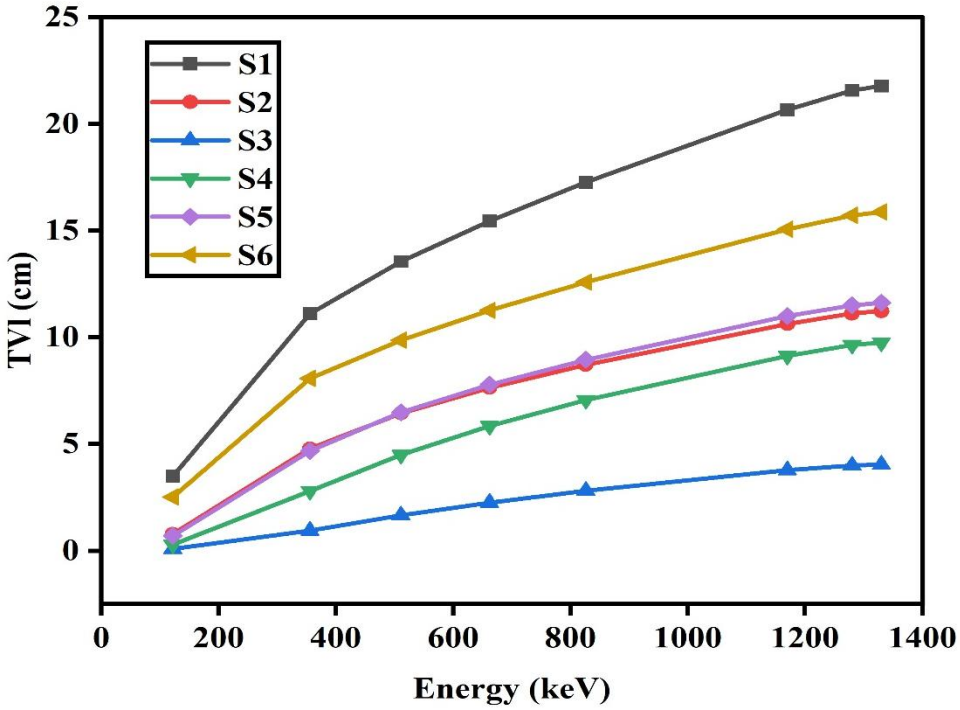

Fig. 5 Tenth Value Layer (TVL) of Transition Metal Salts.

4.Conclusions

Many different materials can be used to reduce gamma radiation. Understanding how γ-rays attenuate due to photon-matter interactions might help select the appropriate shielding material for a certain application. As this understanding grows and the physical, chemical, and economic restrictions are taken into account, resources will be used more effectively to construct the most suited types of shielding.

To determine if Transition Metal Salts may be utilized as a radiation shield, the gamma ray shielding parameters μm, μ, $X_{1/2}$, and $X_{1/10}$ were tested theoretically and experimentally. The XCOM program was used to simulate these characteristics for the samples under examination. The S1 sample has the highest HVL but the least optimum shielding ability, while the S3 sample has the lowest HVL but the best shielding ability.

5. References

1. Celal Avcıoğlu, and Suna Avcıoğlu, Transition Metal Borides for All-in-One Radiation Shielding, Materials 2023, 16, 6496.
2. Hussein, E.M. Abou, Madbouly, A.M., Eldin, F.M. Ezz, ElAlaily, N.A, Evaluation of physical and radiation shielding properties of Bi2O3–B2O3 glass doped transition metals ions, matchemphys.2020.124212.
3. Ahmed S.K., Keole S.R. Proton Therapy in the Adolescent and Young Adult Population. Cancers. 2023; 15:4269.
4. Fernández-Arias P., Vergara D., Antón-Sancho Á. Global Review of International Nuclear Waste Management. Energies. 2023; 16:6215.
5. Moriarty P., Honnery D. Review: The Energy Implications of Averting Climate Change Catastrophe. Energies. 2023; 16:6178.

6. Sidhu A., Khan N., Phillips C., Briones J., Kapoor A., Zalewski P., Fleshner N.E., Chow E., Emmenegger U. Prevalence and Prognostic Implications of PSA Flares during Radium-223 Treatment among Men with Metastatic Castration Resistant Prostate Cancer. J. Clin. Med. 2023; 12:5604.
7. Tuieng R.J., Cartmell S.H., Kirwan C.C., Sherratt M.J. The Effects of Ionising and Non-Ionising Electromagnetic Radiation on Extracellular Matrix Proteins. Cells. 2021; 10:3041.
8. Poltabtim, W, Wimolmala, E, Saenboonruang, K. Properties of lead-free gamma-ray shielding materials from metal oxide/EPDM rubber composites. Radiat. Phys. Chem. 2018, 153, 1−9.
9. (Li, Q, Wang, Y, Xiao, X.; Zhong, R, Liao, J, Guo, J, Liao, X, Shi, B. Research on X-ray shielding performance of wearable Bi/Ce natural leather composite materials. J. Hazard. Mater. 2020, 398, 122943.
10. Cheraghi, E, Chen, S.; Liu, J. A, Sun, Y, Yeow, J. T. W. Lightweight and flexible bismuth oxide composite with enhanced x ray shielding efficiency. J. Appl. Polym. Sci. 2022, 139 (45), No. e53130.
11. Mesbahi, A, Ghiasi, H. Shielding properties of the ordinary concrete loaded with micro- and nano-particles against neutron and gamma radiations. Appl. Radiat. Isot. 2018, 136, 27−31.
12. Tiamduangtawan, P, Wimolmala, E.; Meesat, R, Saenboonruang, K. Effects of Sm2O3 and Gd2O3 in poly (vinyl alcohol) hydrogels for potential use as self-healing thermal neutron shielding materials. Radiat. Phys. Chem. 2020, 172, 108818.
13. Kaur, T.; Sharma, J.; Singh, T. Review on scope of metallic alloys in gamma rays shield designing. Prog. Nucl. Energy 2019, 113, 95–113.
14. Kharita, M.H.; Yousef, S.; AlNassar, M. Review on the addition of boron compounds to radiation shielding concrete. Prog. Nucl. Energy 2011, 53, 207–211.
15. Kavaz, E, Ersundu, M.Ç.; Ersundu, A.E, Tekin, H.O. Synthesis and characterization of newly developed phosphate-based glasses through experimental gamma-ray and neutron spectroscopy methods: Transmission and dose rates. Ceram. Int. 2022, 48, 13842–13849.
16. Ilik, E, Kavaz, E, Kilic, G, Issa, S.A.M, Zakaly, H.M.H, Tekin, H.O. A closer-look on Copper (II) oxide reinforced Calcium-Borate glasses: Fabrication and multiple experimental assessment on optical, structural, physical, and experimental neutron/gamma shielding properties. Ceram. Int. 2022, 48, 6780–6791.
17. Al-Ghamdi,H.;Almuqrin,A.H, Koubisy, M.S.I, Mahmoud, K.A, Sayyed, M.I, Darwish, M.A Henaish, A.M.A. Zinc-lead-borate glasses doped with dysprosium oxide: Structure, optical, and radiation shielding features. Optik 2021, 246, 167765.
18. Kavaz, E, Ilik, E.; Kilic, G, ALMisned, G,Tekin, H.O. Synthesis and experimental characterization on fast neutron and gamma ray attenuation properties of high-dense and transparent Cadmium oxide (CdO) glasses for shielding purposes. Ceram. Int. 2022, 48, 23444–23451.
19. Lakshminarayana, G, Elmahroug, Y, Kumar, A, Tekin, H.O, Rekik, N Dong, M, Lee, D.-E, Yoon, J.; Park, T. Detailed Inspection of-ray, Fast and Thermal Neutrons Shielding Competence of Calcium Oxide or Strontium Oxide Comprising Bismuth Borate Glasses. Materials 2021, 14, 2265.

20. ALMisned, G, Tekin, H.O.; Kavaz, E, Bilal, G, Issa, S.A.M, Zakaly, H.M.H, Ene, A. Gamma, Fast Neutron, Proton, and Alpha Shielding Properties of Borate Glasses: A Closer Look on Lead (II) Oxide and Bismuth (III) Oxide Reinforcement. Appl. Sci. 2021, 11, 6837.
21. Sallam, O.I, Madbouly, A.M, Moussa, N.L, Abdel-Galil, A. Impact of radiation on CoO-doped borate glass: Lead-free radiation shielding. Appl. Phys. A 2022, 128, 70.
22. Kalidas B Gaikwad, Ketan P Gattu, Shamsan S Obaid, Pravina P Pawar, Comparative study of radiation shielding parameters for $NiFe_2O_4$ and $CoFe_2O_4$ nanoparticles, AIP Conference Proceedings, 3149,2024.
23. Balci, S., Sefa, I., Altin, N., 2016. An investigation of ferrite and nanocrystalline core materials for medium-frequency power transformers. J. Electron. Mater. 45 (8), 3811–3821.
24. Hezam, F. A., Khalifa, N. O., Nur, O., & Mustafa, M. A. (2021). Synthesis and magnetic properties of Ni0. 5MgxZn0. 5-xFe2O4 (0.0≤ x≤ 0.5) nanocrystalline spinel ferrites. Materials Chemistry and Physics, 257, 123770.
25. Akhtar, M. N., Rahman, A., Sulong, A. B., & Khan, M. A. (2017). Structural, spectral, dielectric and magnetic properties of Ni0. 5MgxZn0. 5-xFe2O4 nanosized ferrites for microwave absorption and high frequency applications. Ceramics International, 43(5), 4357-4365.
26. Dinesh Varshney, Kavita Verma, substitutional effect on structural and dielectric properties of Ni1-xAxFe2O4(A ¼ Mg, Zn) mixed spinel ferrites, materials chemistry and Physics,140(2013),412-418.
27. Akkurt I, Tekin HO Radiological Parameters for bismuth oxide Glasses using Phy-X/PSD software. Emerg Mater Res 9(3):1020–1027.
28. M.I. Sayyed, Ferdi Akman and Mustafa Recep Kaçal, Experimental investigation of photon attenuation parameters for different binary alloys, Radiochim. Acta; 107(4) (2019) 339–348.
29. Kalidas B. Gaikwad, Ketan P. Gattu, Chaitali V. More, Pravina P. Pawar, Physical, structural and nuclear radiation shielding behaviour of Ni–Cu–Zn Fe2O4 ferrite nanoparticles, Applied Radiation and Isotopes, 207, (2024), 111244.
30. Shamsan S, Obaid MI, Sayyed DK, Gaikwad P, Pawar P Attenuation coefficients and exposure buildup factor of some rocks for gamma ray shielding applications. Radiat Phys Chem 148:86–94. (2018)
31. Kalidas B. Gaikwad, Ketan P. Gattu, Shamsan S. Obaid, Pravina P. Pawar, Comparative study of radiation shielding parameters for $NiFe_2O_4$ and $CoFe_2O_4$ nanoparticles, AIP Conf. Proc. 3149, 020014 (2024).
32. S. S. Obaid, D. K. Gaikwad and P. P. Pawar, Determination of gamma ray shielding parameters of rocks and concrete, Radiat. Phys. Chem., 2018, 144, 356–360.
33. El-Agawany FI, Tashlykov OL,Mahmoud KA, Rammah YS The radiation shielding properties of ternary SiO2–SnO–SnF2 glasses: simulation and theoretical study. Ceram Int 46:23369–23378. (2020)

34. Kalidas B. Gaikwad, Ketan P. Gattu, Chaitali V. More, Hasan Ogul, Pravina P. Pawar, Gamma-ray shielding features of $Co_{1-x}Cu_xFe_2O_4$ ferrite: A combined experimental, theoretical and simulation investigation, Radiation Physics and Chemistry,224,111996, (2024).
35. Kalidas B. Gaikwad, Ketan P. Gattu, Chaitali V. More, M.I. Sayyed, Kanchan R. Niras, Pravina P. Pawar, Experimental evaluation of gamma radiation attenuation properties of $Ni_{0.2}Mg_XZn_{0.8-X}Fe_2O_4$, Optical Materials 148 (2024) 114807.
36. Kalidas B Gaikwad, Merfat Algethami, Chaitali V More, MI Sayyed, Pravina P Pawar, Enhanced radiation shielding properties of advanced ceramic materials, Journal of Alloys and Compounds, Volume 1033, 20 June 2025, 181384.